



Cite this: DOI: 10.1039/c8nj06491a

# A direct comparison of monomeric vs. dimeric and non-annulated vs. *N*-annulated perylene diimide electron acceptors for organic photovoltaics†

 Maryam Nazari,<sup>id</sup> Edward Cieplechowicz,<sup>id</sup> Thomas A. Welsh<sup>id</sup> and Gregory C. Welch<sup>id</sup>\*

Herein we report on four perylene diimide (PDI) variants to study the effects that *N*-annulation and dimerization have on optoelectronic properties and organic solar cell device performance. The PDI compounds were synthesized following a scalable and efficient procedure and studied by cyclic voltammetry, solution and solid-state optical absorption spectroscopy, emission spectroscopy, and density functional theory analysis. The thin-film morphology was probed by optical and atomic force microscopy. Dimerization stabilized the frontier molecular orbital energy levels and reduced aggregation in the thin-films. *N*-Annulation resulted in a destabilization of the frontier molecular orbital energy levels in both the monomers and dimers and enabled the formation of smoother films with smaller domain sizes. Each PDI molecule was evaluated as a non-fullerene acceptor in bulk-heterojunction solar cells using the donor polymers PTB7-Th and PffBT4T-2OD. The dimers outperformed the monomers, while *N*-annulated PDIs led to devices with higher open-circuit voltages.

Received 24th December 2018,  
Accepted 2nd March 2019

DOI: 10.1039/c8nj06491a

rsc.li/njc

## Introduction

Functional organic  $\pi$ -conjugated molecules and polymers have been widely used as active materials in photovoltaic devices.<sup>1–4</sup> Ease of synthetic modification to the  $\pi$ -conjugated backbone and periphery functional groups allows for facile tuning of physical, optical, and electronic properties, which enables tailored device properties that can lead to improved performance.<sup>5–8</sup> Molecules and polymers based on thiophenes<sup>9,10</sup> and/or dye materials<sup>11–13</sup> have been most commonly used in solution processed bulk-heterojunction (BHJ) organic solar cells (OSCs) owing to their optoelectronic properties being well suited to visible light absorption and charge transfer. Over the past few years, the power conversion efficiency (PCE) of OSCs has dramatically improved with current records of > 14% for single-junction<sup>14</sup> and > 15% for tandem devices.<sup>15,16</sup>

Many OSCs use fullerene acceptors owing to excellent electron transport properties and tendency to form organized nano-aggregates in BHJ films.<sup>17–19</sup> However, fullerenes suffer from several disadvantages including poor visible light absorption, lack of energy level tunability, photochemical instability, and difficulty in synthesis and purification.<sup>20,21</sup> For these reasons,

non-fullerene acceptors (NFAs) have been extensively studied in recent years.<sup>8,14,15,22–27</sup> Indacenodithiophene-based compounds (IDTs) have proved quite effective owing to strong low-energy optical absorption and good miscibility with donor polymers leading to favorable phase separated BHJ morphologies.<sup>28–30</sup> Indeed IDT-based OSCs exhibit remarkably high fill factors (FF).<sup>30–32</sup> However, high performing IDT-based NFAs typically require multiple synthetic steps, which makes large scale production more difficult.<sup>33</sup> An alternative to IDT based NFAs are those based on perylene diimides (PDIs), which are easily synthesized and modified *via* simple chemical reactions from cheap and abundant dyes and pigments.<sup>13,34–37</sup> They exhibit strong light absorption in the blue-green region of the visible spectrum, have deep electronic energy levels, and are good electron transport materials making them compatible with nearly all low-band gap hole transporting polymers. Indeed, polymer-based OSCs that use dimeric or tetrameric PDI NFAs have achieved > 9%<sup>38</sup> and > 10%<sup>39</sup> PCE, respectively.

The PDI chromophore is quite versatile as it can be easily functionalized at the bay, headland, and/or imide positions to tune molecular and bulk properties (Fig. 1). A common method of functionalization of PDI is to dimerize at the bay position. One such PDI dimer has achieved PCE of up to 6% in OSC devices.<sup>40</sup> Another common functionalization is heteroatom annulation at the bay position, which has been an effective strategy to control the solubility, self-assembly, and optoelectronic properties of PDI materials. For OSC applications, PDI dimers with S and Se

Department of Chemistry, University of Calgary, 2500 University Drive N.W., Calgary, Alberta, T2N 1N4, Canada. E-mail: gregory.welch@ucalgary.ca;  
Tel: +1-403-210-7603

† Electronic supplementary information (ESI) available. See DOI: 10.1039/c8nj06491a

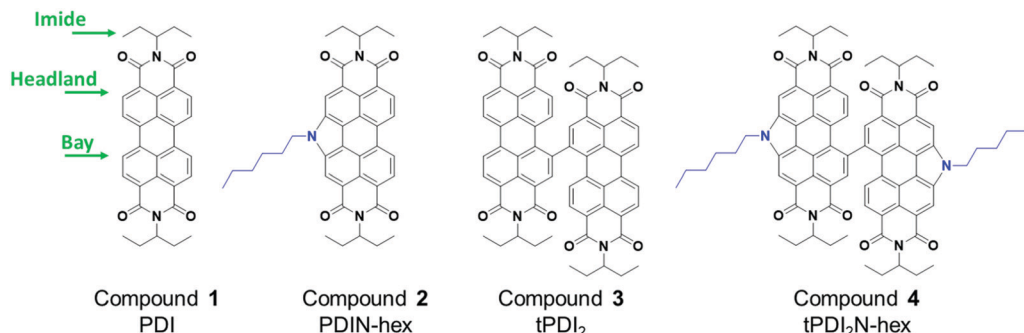


Fig. 1 Functionalization points for the PDI chromophore and chemical structures of the PDI materials directly compared in this study.

annulation have been reported with PCEs above 7% and 8%, respectively.<sup>41,42</sup> In our group, we have focused on *N*-annulated PDI compounds,<sup>43–46</sup> which, in addition to tuning the optoelectronic properties like S and Se annulation, provides an additional handle for functionalization to tune solubility and self-assembly.<sup>45,47–51</sup> OSC devices with PCEs above 7% have been achieved using these *N*-annulated PDI NFAs.<sup>52</sup>

While investigating the *N*-annulated PDI dimers over the past few years, we noticed that there has never been a direct comparison between non-annulated PDI and *N*-annulated PDI monomers and dimers for OSCs. It is important to fully study the impact of such structural changes to gain a greater understanding of how these molecules function in OSC devices. This study serves to fill that gap and provides a structure–property–functional relationship study. The structures of PDI acceptors used in this study are shown in Fig. 1. Compounds 1, 2, and 4

have been reported previously while compound 3 is new. Full synthetic details can be found in the ESI.†

## Optical properties

The solution and film optical absorption properties of compounds 1, 2, 3, and 4 were determined using UV-vis spectroscopy (Fig. 2). The solution spectra of the monomers (1 and 2) exhibit characteristic transitions for PDI based materials. They exhibit absorption from 400–550 nm with three distinct bands for the 0-0, 0-1 and 0-2 vibronic transitions.<sup>53</sup> A transition from solution to film reveals differences between the two compounds. For 1 the onset of absorption is red-shifted by  $\Delta 72$  nm to 627 nm, while 2 is only red-shifted by  $\Delta 48$  nm to 606 nm. The difference implies weaker intermolecular coupling in films of 2 vs. 1, attributed to the presence of the *N*-alkyl functional group.

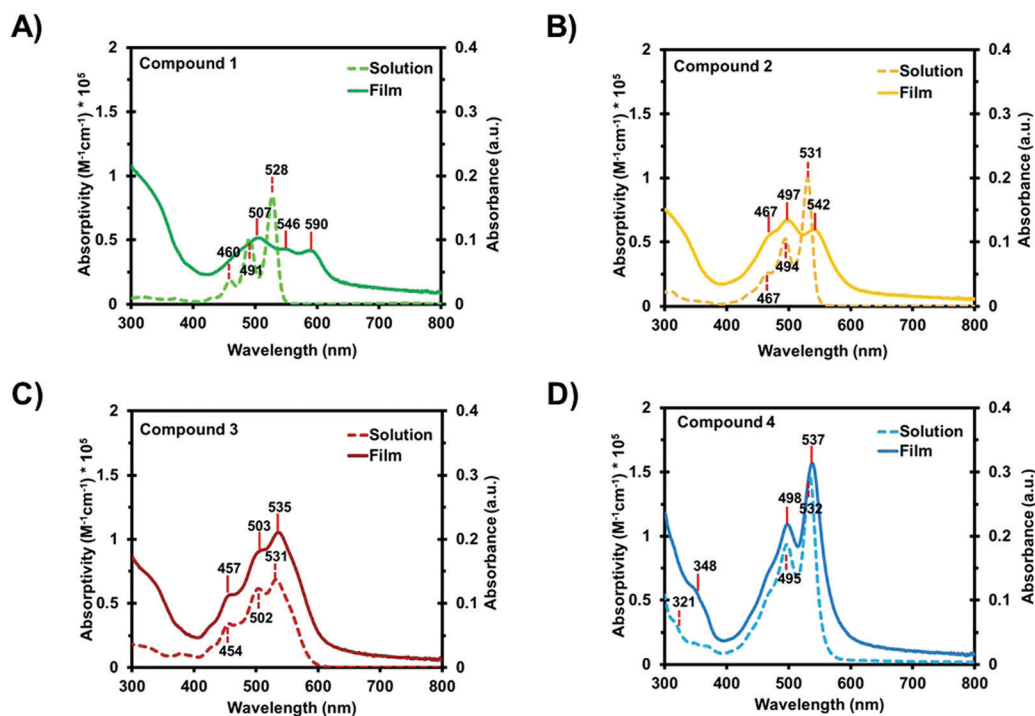


Fig. 2 UV-visible spectra of PDI materials (A) 1, (B) 2, (C) 3, and (D) 4 in  $C_6H_5Cl$  solution ( $0.01 \text{ mg mL}^{-1}$ ) and as 'as-cast' films spin-coated from  $C_6H_5Cl$  solutions ( $10 \text{ mg mL}^{-1}$ ) onto glass substrates under identical conditions. Left y-axis = solution. Right y-axis = film.

**Table 1** Optical and electrochemical data for compounds **1**, **2**, **3**, and **4** in solution and as thin-films

Compound	<b>1</b> <sup>52</sup>	<b>2</b> <sup>52</sup>	<b>3</b>	<b>4</b> <sup>52</sup>
Solution Abs max (nm)	528	531	535	537
Solution Abs onset (nm)	555	558	605	577
Molar absorptivity (M <sup>-1</sup> cm <sup>-1</sup> )	84 000	100 000	69 000	147 000
Solution Em max (nm)	578	580	612	588
Solution quantum yield (nm)	91	64	10	60
Film Abs max (nm)	507	497	535	537
Film Abs onset (nm)	627	606	621	617
Film Em max (nm)	615	n/a	n/a	633
<i>E</i> <sub>1/2</sub> oxidation (V)	n/a	1.09	n/a	1.14
Oxidation onset (V)	n/a	1.01	n/a	1.03
Ionization potential (eV)	n/a	5.89	n/a	5.94
<i>E</i> <sub>1/2</sub> 1st reduction (V)	-1.15	-1.30	-1.04	-1.29
Reduction onset (V)	-1.06	-1.21	-1.02	-1.16
Electron affinity (eV)	3.65	3.50	3.76	3.51

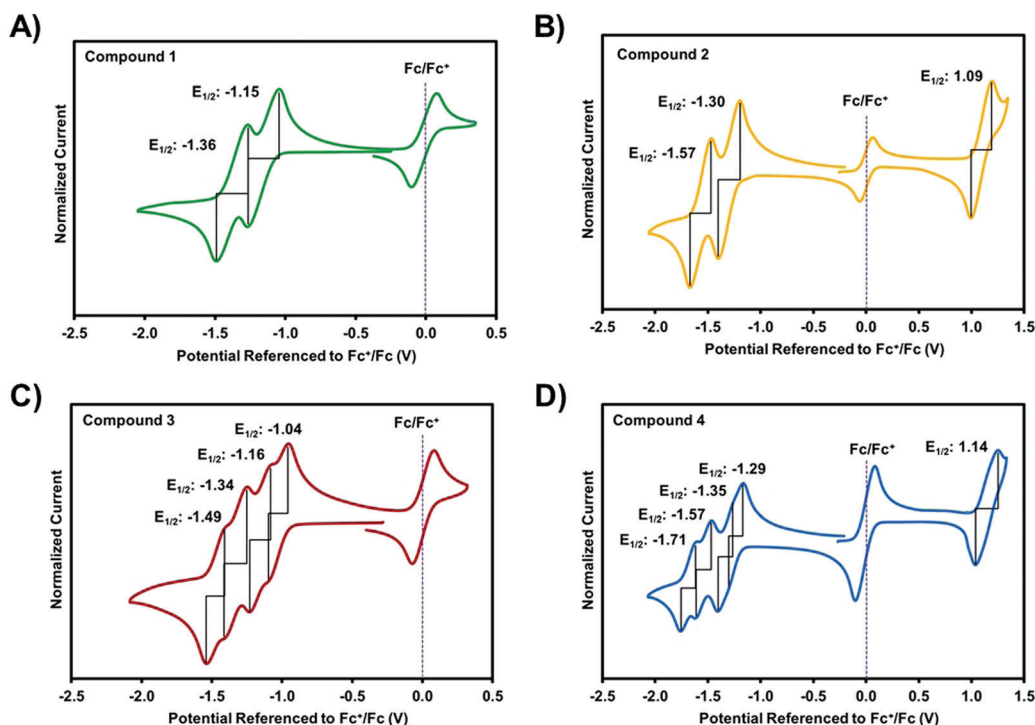
The solution spectra of the dimers (**3** and **4**) are different from their monomeric analogues. While compound **3** exhibits similar absorption from 400–500 nm with three distinct transitions, the absorption band is broadened and the absorption peaks less sharp. The onset of absorption is also red-shifted compared to **1**. The features of compound **3** are nearly identical to a similar PDI dimer with longer alkyl chains off the imide N-atoms.<sup>54,55</sup> The solution spectra of **4** is the most different with only two distinct vibronic transitions, with the 0-0 (*ca.* 537 nm) transition the most intense. Such differences can be attributed to the more isotropic shape of the dimeric compounds leading to different intra and intermolecular electronic interactions. Of note the solution spectra of each compound do not change upon heating implying no significant aggregation in solution (Fig. S6, ESI<sup>†</sup>). The thin-film

spectra of **3** and **4** are only slightly red-shifted from the solution spectra, much less than their monomeric analogues, consistent with less intermolecular coupling in these systems owing to the non-planar geometries.<sup>56,57</sup> All optical absorption data are listed in Table 1.

The photoluminescence (PL) spectra of all compounds were measured in solution and film (Table 1 and Fig. S7, ESI<sup>†</sup>). Solutions of compounds **1**, **2**, **3**, and **4** show emission maxima at 578, 580, 612, and 588 nm, respectively, and have shapes typical of PDI materials. Both the monomers **1** and **2** have two emission bands while the dimers have only one. Quantum yields were measured to be 91, 64, 10, and 60% for compounds **1**, **2**, **3**, and **4** solutions in C<sub>6</sub>H<sub>5</sub>Cl, respectively. Compound **3** has the largest Stokes shift and lowest quantum yield indicating significant non-radiative energy loss, an unusual phenomenon.

## Electrochemical properties

The electrochemical properties of the PDI materials were determined using solution cyclic voltammetry (Fig. 3 and Fig. S8, ESI<sup>†</sup>). All compounds exhibit fully reversible reduction waves. The monomers **1** and **2** exhibit two reduction waves while the dimers **3** and **4** exhibit four reduction waves, which is typical for PDI monomers and dimers, as the PDI chromophore is stable as a radical dianion.<sup>41,52,54</sup> The *N*-annulated compounds **2** and **4** exhibited two reversible oxidation waves while compounds **1** and **3** did not reversibly oxidize, consistent with the literature.<sup>52,54</sup> Oxidation occurs at the electron rich pyrrole ring at the bay position in **2** and **4**. The *E*<sub>1/2</sub> oxidation and reduction potentials

**Fig. 3** Cyclic voltammograms (with ferrocene internal standard) of PDI materials (A) **1**, (B) **2**, (C) **3**, and (D) **4** with *E*<sub>1/2</sub> potentials shown.

for each compound were used to experimentally determine the ionization potential (IP) and electron affinity (EA) energies, respectively, which correspond to theoretical HOMO and LUMO energy levels (Table 1). A conversion factor of 4.8 eV (accepted HOMO energy level of ferrocene) was used.<sup>58</sup>

*N*-Annulation has a large effect on the reduction potentials for PDI. Compounds **2** (*ca.*  $-1.30$  V) and **4** (*ca.*  $-1.29$  V) have significantly more negative  $E_{1/2}$  reduction potentials than in their counterparts **1** (*ca.*  $-1.15$  V) and **3** (*ca.*  $-1.04$  V). As a result, the EA of **2** and **4** is decreased compared to **1** and **3**. This is a powerful example of how *N*-annulation of PDI can influence and tune the electrochemical properties by increasing the electron density within the polycyclic aromatic core. This has a consequence for OSC devices in terms of increased open-circuit voltages. The differences in electronic energy levels were confirmed using DFT and TD-DFT calculations (Fig. S10 and Table S1, ESI†).

## Thin-film morphology

The thin-film morphology of compounds **1**, **2**, **3**, and **4** were investigated using polarized optical microscopy (POM) and atomic force microscopy (AFM) (Fig. 4). All films were spin-coated from  $10 \text{ mg mL}^{-1}$   $\text{C}_6\text{H}_5\text{Cl}$  solutions onto cleaned glass substrates under identical conditions. All compounds formed uniform films but with very different roughness and domain sizes. The non-annulated PDI monomer **1** formed highly aggregated films with large domains upwards of  $1000 \text{ nm}$  in width (Fig. 4A). The *N*-annulated PDI monomer **2** also formed aggregated films but with smaller more fibril like domains ranging from  $300\text{--}500 \text{ nm}$  in width. These aggregated films are consistent with literature findings for monomeric PDIs which are well known to self-assemble into organized nanostructures in the solid-state *via* strong  $\pi\text{--}\pi$  interactions.<sup>59</sup> A major difference is seen with the PDI dimers. Both compounds **3** and **4** form very smooth films with small domain sizes. The film of **3** shows

fibril like features of several hundred nanometers in size, while the film of **4** is nearly feature less. These results confirm the long-standing notion that dimerization of PDI chromophores reduces aggregation and that the introduction of an *N*-hexyl chain further reduces the tendency of the PDI chromophores to form aggregated solid-state morphologies with large features. For OSCs, smaller, less aggregated domains usually lead to best performance. Thus, the *N*-annulated dimer is expected to yield the best photovoltaic devices.

## Organic solar cells

Due to the critical role of donor/acceptor pairings in the efficiency of the device, OSC devices were fabricated under identical conditions with compounds **1**, **2**, **3**, and **4** using two different polymer donors (Fig. 5). PTB7-Th and PffBT4T-2OD, also referred to as PCE10 and PCE11, respectively, were selected as they have complementary optical absorption (*ca.*  $400\text{--}800 \text{ nm}$ ), appropriately offset electronic energy levels, and are proven to yield good PCE devices with PDI based NFAs.<sup>45,60,61</sup> Due to ease of fabrication and greater environmental stability,<sup>62</sup> OSCs were fabricated using an air-processed and air-tested inverted geometry: ITO/ZnO/BHJ/MoO<sub>x</sub>/Ag.<sup>63</sup>

BHJ films using the donor polymers PTB7-Th and PffBT4T-2OD were fabricated from  $\text{C}_6\text{H}_5\text{Cl}$  solutions ( $10 \text{ mg mL}^{-1}$ ) using a 1:1 polymer:PDI weight ratio. The active layers were spin-cast in the air, with room temperature solutions and substrates, without additives or any post-deposition treatments. Controlled processing conditions were used to ensure a direct comparison of the PDI materials. We fully recognize that solar cell performance can be improved through processing optimization but that was beyond the scope of this study. Tabulated data for all devices is given in Table 2. Current-voltage curves and graphical metric comparison for PTB7-Th:PDI and PffBT4T-2OD:PDI based OSCs are shown in Fig. 6.

The optical absorption spectra of PTB7-Th:PDI films (Fig. S11A, ESI†) exhibit absorption from  $400\text{--}800 \text{ nm}$  whereas those of

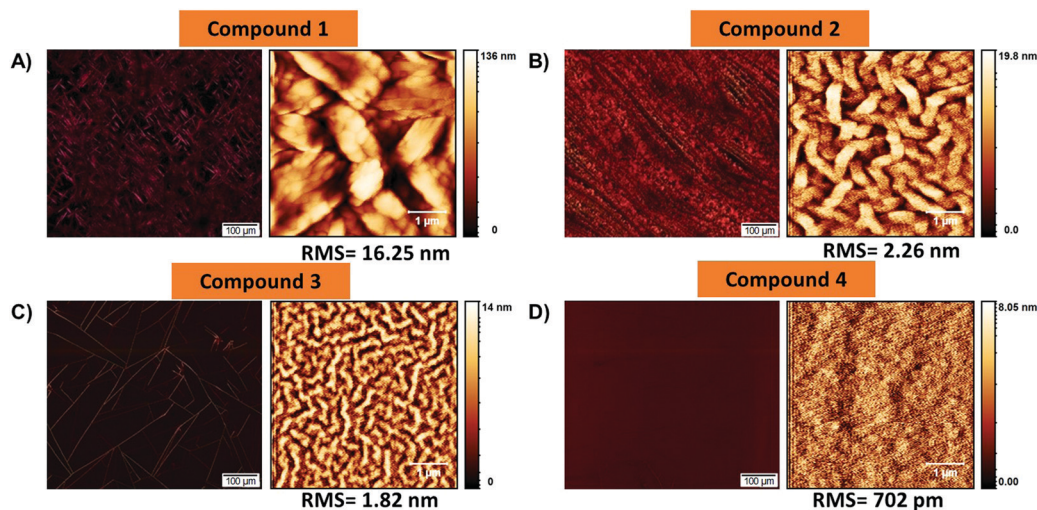


Fig. 4 Polarized optical microscopy (POM) and atomic force microscopy (AFM) images of PDI materials (A) **1**, (B) **2**, (C) **3**, (D) **4** as 'as-cast' films spin-coated from  $\text{C}_6\text{H}_5\text{Cl}$  solutions.

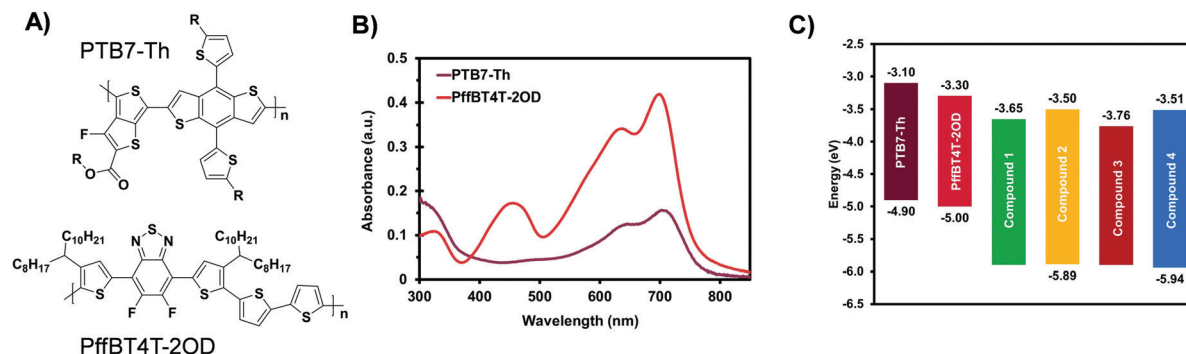


Fig. 5 (A) Chemical structures of donor polymers PTB7-Th and PffBT4T-2OD used to make BHJ organic solar cells. R = 2-ethylhexyl. (B) Optical absorption spectra of PTB7-Th and PffBT4T-2OD films spin-cast from 5 mg mL<sup>-1</sup> under identical conditions. The lower absorption intensity of PTB7-Th reflects its lower solution viscosity. (C) Energy level plot of the polymer donors and PDI acceptors. Values estimated from CV data obtained in our labs (Fig. S8, ESI<sup>†</sup>). HOMO energy levels of **1** and **3** could not be determined by CV.

Table 2 Photovoltaic parameters for PTB7-Th:**1,2,3,4**<sup>a</sup> and PffBT4T-2OD:**1,2,3,4**<sup>b</sup> based organic solar cells<sup>c</sup>

Parameters	$V_{OC}$ (V) avg. (best)	$J_{sc}$ (mA cm <sup>-2</sup> ) avg. (best)	FF (%) avg. (best)	PCE (%) avg. (best)
PTB7-Th: <b>1</b>	0.81 (0.81)	10.3 (11.5)	40.8 (43.2)	3.40 (4.00)
PTB7-Th: <b>2</b>	0.98 (1.00)	7.0 (7.4)	33.3 (35.1)	2.29 (2.60)
PTB7-Th: <b>3</b>	0.73 (0.75)	10.3 (10.4)	51.6 (52.3)	3.86 (4.07)
PTB7-Th: <b>4</b>	0.97 (0.99)	12.1 (12.4)	46.9 (46.9)	5.51 (5.72)
PffBT4T-2OD: <b>1</b>	0.78 (0.80)	3.8 (4.5)	41.6 (44.3)	1.25 (1.59)
PffBT4T-2OD: <b>2</b>	0.95 (0.98)	3.7 (4.0)	41.1 (43.0)	1.45 (1.69)
PffBT4T-2OD: <b>3</b>	0.78 (0.79)	9.6 (9.8)	47.7 (47.4)	3.59 (3.66)
PffBT4T-2OD: <b>4</b>	1.02 (1.03)	7.3 (8.3)	40.9 (42.1)	3.06 (3.59)

<sup>a</sup> Active layers were spin cast at 1500 rpm from 10 mg mL<sup>-1</sup> solutions in CB (1 : 1 blend ratio). <sup>b</sup> Active layers were spin cast at 1200 rpm from 10 mg mL<sup>-1</sup> solutions in CB. (1 : 1 blend ratio). <sup>c</sup> Device architecture: ITO/ZnO/BHJ/MoO<sub>x</sub>/Ag.

PffBT4T-2OD:PDI films (Fig. S12A, ESI<sup>†</sup>) exhibit absorption from 350–750 nm, both suitable for solar photon harvesting. For all films (except PffBT4T-2OD:**1**) the emission of the polymer donor was efficiently quenched by the PDI acceptor indicating electron transfer occurs in the BHJ films. PL spectra of blended films are given in the ESI<sup>†</sup> (Fig. S11B and S12B). The lack of PL quenching in the film of PffBT4T-2OD:**1** is explained by the large phase separated surface seen in the AFM image (Fig. 13A, ESI<sup>†</sup>). Lack of donor-acceptor interface interaction inhibits electron transfer.

OSCs with PTB7-Th:**1** active layer had average PCE of 3.4%. This performance is on par with related solar cells using monomeric PDIs.<sup>64,65</sup> OSCs using the *N*-annulated PDI **2** had a reduced average PCE of 2.3%. Despite the lower PCE, PTB7-Th:**2** OSCs had a higher  $V_{OC}$  because of the raised LUMO level of compound **2** leading to a larger energy gap between the polymer HOMO energy level and acceptor LUMO energy level. PTB7-Th:**3** based OSCs had an average PCE of 3.9% while PTB7-Th:**4** based OSCs had average PCE of 5.5%. Consistent with the comparison of **1** vs. **2**, the OSCs based on **4** had higher  $V_{OC}$  than those based on **3**. Again, a result of *N*-annulation destabilizing the PDIs LUMO energy level. Although devices based on **4** had slightly lower fill factors compared to **3** based devices, higher PCEs were obtained owing to a higher  $V_{OC}$  and  $J_{SC}$ . The best PCE of 5.5% for PTB7-Th:**4** OSCs is consistent with literature results.<sup>46–48,52,66,67</sup>

OSCs with PffBT4T-2OD:**1** active layer gave an average PCE of 1.25%. The OSCs with BHJ active layers using the *N*-annulated

monomer **2** gave slightly higher efficiency (*ca.* 1.45%) due to the higher  $V_{OC}$  (0.95 V vs. 0.78 V). Use of the dimeric PDI acceptors led to higher PCEs of 3.59% and 3.06%, respectively, for PffBT4T-2OD:**3** and PffBT4T-2OD:**4** based OSCs. Although devices based on *N*-annulated PDI dimer **4** gave slightly lower efficiency due to the lower short-circuit current and FF ( $J_{SC} = 7.34$  mA cm<sup>-1</sup>, FF = 40.31%), using compound **4** lead to significantly higher  $V_{OC}$  (0.78 V for PffBT4T-2OD:**3** films vs. 1.02 V for PffBT4T-2OD:**4** films).

In general, use of the *N*-annulated PDI materials (**2** and **4**) lead to solar cells with significantly higher  $V_{OC}$ , over 200 mV on average, compared to the non-annulated PDI materials (**1** and **3**). This result highlights the positive impact of *N*-annulation on the electronic properties of the PDI that results in improved solar cell device characteristics. Furthermore, use of the dimeric compounds (**3** and **4**) resulted in better performing OSCs than those based on the monomeric analogues (**1** and **2**), emphasizing the long-standing notion that best PDI NFAs should be comprised of two or more PDI chromophores.

To help rationalize these results, the surface morphology was analysed using AFM. Phase and height images are shown in Fig. S12 and S13 (ESI<sup>†</sup>). BHJ blends using compound **1** had a high surface roughness (RMS = 7 nm for PTB7-Th blends and RMS = 17 nm for PffBT4T-2OD blends) owing to the stronger aggregation tendencies of the planar PDI. Domain sizes were on the order of microns, not suitable for efficient charge separation,

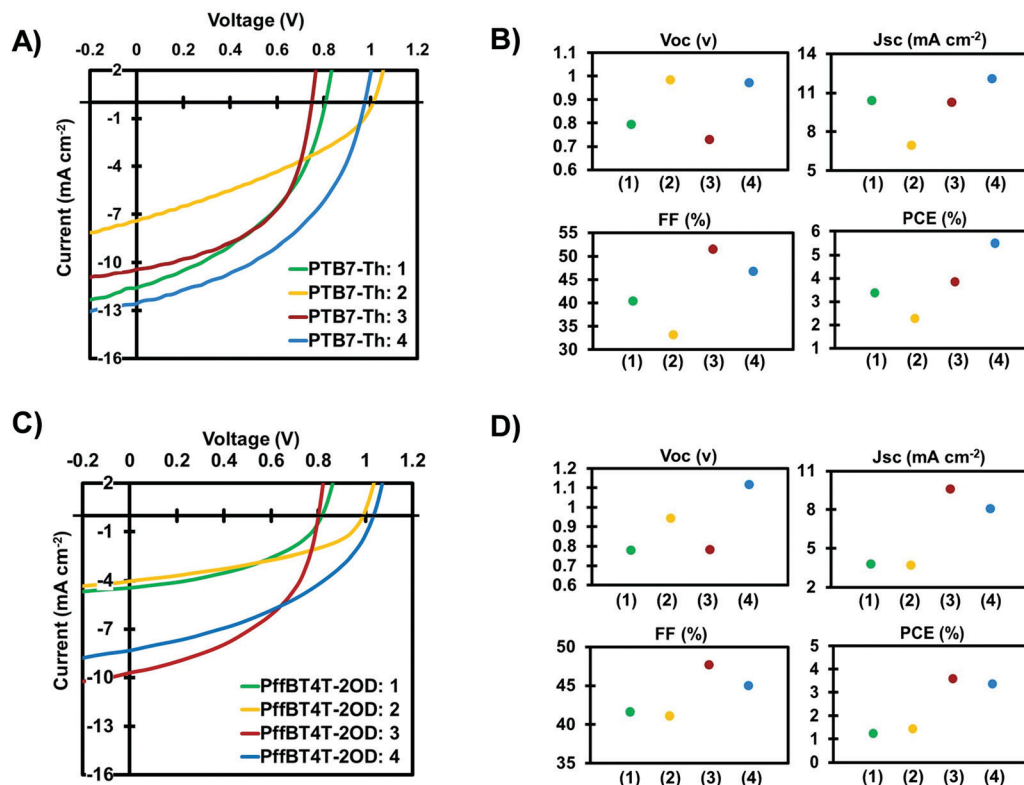


Fig. 6 Current voltage-curves and metrical graphs for PTB7-Th:PDI (A and B) and PffBT4T-2OD:PDI (C and D) based organic solar cells.

thus the overall lower PCE. Blends using compound 2 had much smoother films ( $\text{RMS} < 3 \text{ nm}$ ) but appeared to be very intermixed based on the uniform and featureless phase images. The lack of order and phase separation may explain the poor FF leading to the low PCE. Thus, while the *N*-annulation is favourable for improving the energetics of the blends (*i.e.* increased  $V_{oc}$ ), the additional *N*-hexyl group seems to impede phase-separation and molecular organization lowering (*i.e.* lower  $J_{sc}$  and FF), in the monomeric systems. All blends using the dimeric PDI materials exhibited smooth uniform films but with more defined features than that of compound 2. Blends films using 3 or 4 are very similar, and this reflects the similar  $J_{sc}$  and FF seen on all OSCs using these acceptors. Once again, the biggest difference in device performance is a result of the  $V_{oc}$  and the relative electronic energy levels of the materials.

## Conclusion

In this contribution we have compared four different PDI molecular materials relevant to the field of organic photovoltaics. The impact of *N*-annulation at the bay position of the PDI chromophore and dimerization of the PDI chromophore were evaluated. We have shown that *N*-annulation serves to both decrease the electron affinity of the PDI and the tendency of the PDI to form large aggregates in the film. Dimerization of the PDI chromophore reduces the tendency of the materials to aggregate in the film with the *N*-annulated PDI dimer exhibiting the smoothest films. In terms of OSC performance, all PDI materials

were tested as non-fullerene acceptors with two different donor polymers in inverted single-junction bulk heterojunction devices. In all cases OSCs using the *N*-annulated PDI materials exhibited higher open circuit voltages by  $\sim 200 \text{ mV}$  when compared to those OSC using the non-annulated PDI materials. This is a clear result of the lower electron affinity of the PDI core afforded by the addition of the electron rich *N*-atom in the bay positions. The dimeric PDI materials gave OSCs with slightly better performance than those fabricated with monomeric PDIs (*ca.*  $\sim 3\text{--}5\%$  PCE *vs.*  $\sim 1\text{--}3\%$  PCE). This was attributed to the fact that the dimeric PDI materials lead to BHJ blends with smooth, well organized films. OSCs based on the donor polymer PTB7-Th and the *N*-annulated PDI acceptor 4 gave best PCE of 5.5% and highlights the potential of this class of materials for the development of high performance, fullerene-free OSCs.

## Conflicts of interest

There are no conflicts to declare.

## Acknowledgements

GCW acknowledges NSERC DG (435715-2013), CFI JELF (34102), CRC, and the UofC. MN and TAW are grateful for UofC Eyes High graduate scholarships. This research was undertaken thanks in part to funding from the Canada First Research Excellence Fund (CFREF).

## References

- 1 L. Bian, E. Zhu, J. Tang, W. Tang and F. Zhang, Recent Progress in the Design of Narrow Bandgap Conjugated Polymers for High-Efficiency Organic Solar Cells, *Prog. Polym. Sci.*, 2012, **37**(9), 1292–1331, DOI: 10.1016/j.progpolymsci.2012.03.001.
- 2 K. A. Mazzi and C. K. Luscombe, The Future of Organic Photovoltaics, *Chem. Soc. Rev.*, 2014, **44**(1), 78–90, DOI: 10.1039/C4CS00227J.
- 3 G. Zhang, J. Zhao, P. C. Y. Chow, K. Jiang, J. Zhang, Z. Zhu, J. Zhang, F. Huang and H. Yan, Nonfullerene Acceptor Molecules for Bulk Heterojunction Organic Solar Cells, *Chem. Rev.*, 2018, **118**(7), 3447–3507, DOI: 10.1021/acs.chemrev.7b00535.
- 4 N. Kaur, M. Singh, D. Pathak, T. Wagner and J. M. Nunzi, Organic Materials for Photovoltaic Applications: Review and Mechanism, *Synth. Met.*, 2014, **190**, 20–26, DOI: 10.1016/j.synthmet.2014.01.022.
- 5 H. S. Vogelbaum and G. Sauvé, Recently Developed High-Efficiency Organic Photoactive Materials for Printable Photovoltaic, *Cells: A Mini Review, Synth. Met.*, 2017, **223**, 107–121, DOI: 10.1016/j.synthmet.2016.12.011.
- 6 G. Sauvé and R. Fernando, Beyond Fullerenes: Designing Alternative Molecular Electron Acceptors for Solution-Processable Bulk Heterojunction Organic Photovoltaics, *J. Phys. Chem. Lett.*, 2015, **6**(18), 3770–3780, DOI: 10.1021/acs.jpcclett.5b01471.
- 7 Y.-J. Cheng, S.-H. Yang and C.-S. Hsu, Synthesis of Conjugated Polymers for Organic Solar Cell Applications, *Chem. Rev.*, 2009, **109**(11), 5868–5923, DOI: 10.1021/cr900182s.
- 8 M. Privado, P. de la Cruz, S. Biswas, R. Singhal, G. D. Sharma and F. Langa, Non-Fullerene All Small Molecule Solar Cell Constructed with a Diketopyrrolopyrrole-Based Acceptor Having Power Conversion Efficiency Higher than 9% and Energy Loss of 0.54 eV, *J. Mater. Chem. A*, 2018, **6**, 11714–11724.
- 9 T. P. Kaloni, P. K. Giesbrecht, G. Schreckenbach and M. S. Freund, Polythiophene: From Fundamental Perspectives to Applications, *Chem. Mater.*, 2017, **29**(24), 10248–10283, DOI: 10.1021/acs.chemmater.7b03035.
- 10 F. Zhang, D. Wu, Y. Xu and X. Feng, Thiophene-Based Conjugated Oligomers for Organic Solar Cells, *J. Mater. Chem.*, 2011, **21**(44), 17590–17600, DOI: 10.1039/C1JM12801A.
- 11 J.-F. Morin, Recent Advances in the Chemistry of Vat Dyes for Organic Electronics, *J. Mater. Chem. C*, 2017, **5**(47), 12298–12307, DOI: 10.1039/C7TC03926C.
- 12 M. Gsänger, D. Bialas, L. Huang, M. Stolte and F. Würthner, Organic Semiconductors Based on Dyes and Color Pigments, *Adv. Mater.*, 2016, **28**(19), 3615–3645, DOI: 10.1002/adma.201505440.
- 13 E. Kozma and M. Catellani, Perylene Diimides Based Materials for Organic Solar Cells, *Dyes Pigm.*, 2013, **98**(1), 160–179, DOI: 10.1016/j.dyepig.2013.01.020.
- 14 Z. Zheng, Q. Hu, S. Zhang, D. Zhang, J. Wang, S. Xie, R. Wang, Y. Qin, W. Li and L. Hong, *et al.*, A Highly Efficient Non-Fullerene Organic Solar Cell with a Fill Factor over 0.80 Enabled by a Fine-Tuned Hole-Transporting Layer, *Adv. Mater.*, 2018, **30**(34), 1801801, DOI: 10.1002/adma.201801801.
- 15 X. Che, Y. Li, Y. Qu and S. R. Forrest, High Fabrication Yield Organic Tandem Photovoltaics Combining Vacuum- and Solution-Processed Subcells with 15% Efficiency, *Nat. Energy*, 2018, **3**(5), 422–427, DOI: 10.1038/s41560-018-0134-z.
- 16 L. Meng, Y. Zhang, X. Wan, C. Li, X. Zhang, Y. Wang, X. Ke, Z. Xiao, L. Ding and R. Xia, *et al.*, Organic and Solution-Processed Tandem Solar Cells with 17.3% Efficiency, *Science*, 2018, eaat2612, DOI: 10.1126/science.aat2612.
- 17 Y. He and Y. Li, Fullerene Derivative Acceptors for High Performance Polymer Solar Cells, *Phys. Chem. Chem. Phys.*, 2011, **13**(6), 1970–1983, DOI: 10.1039/C0CP01178A.
- 18 Y. Liu, J. Zhao, Z. Li, C. Mu, W. Ma, H. Hu, K. Jiang, H. Lin, H. Ade and H. Yan, Aggregation and Morphology Control Enables Multiple Cases of High-Efficiency Polymer Solar Cells, *Nat. Commun.*, 2014, **5**, 5293, DOI: 10.1038/ncomms6293.
- 19 J. Zhao, Y. Li, G. Yang, K. Jiang, H. Lin, H. Ade, W. Ma and H. Yan, Efficient Organic Solar Cells Processed from Hydrocarbon Solvents, *Nat. Energy*, 2016, **1**(2), 15027, DOI: 10.1038/nenergy.2015.27.
- 20 A. F. Eftaiha, J.-P. Sun, I. G. Hill and G. C. Welch, Recent Advances of Non-Fullerene, Small Molecular Acceptors for Solution Processed Bulk Heterojunction Solar Cells, *J. Mater. Chem. A*, 2013, **2**(5), 1201–1213, DOI: 10.1039/C3TA14236A.
- 21 S. M. McAfee, J. M. Topple, I. G. Hill and G. C. Welch, Key Components to the Recent Performance Increases of Solution Processed Non-Fullerene Small Molecule Acceptors, *J. Mater. Chem. A*, 2015, **3**(32), 16393–16408, DOI: 10.1039/C5TA04310G.
- 22 J. Zhang, H. S. Tan, X. Guo, A. Facchetti and H. Yan, Material Insights and Challenges for Non-Fullerene Organic Solar Cells Based on Small Molecular Acceptors, *Nat. Energy*, 2018, **1**, DOI: 10.1038/s41560-018-0181-5.
- 23 C. Yan, S. Barlow, Z. Wang, H. Yan, A. K.-Y. Jen, S. R. Marder and X. Zhan, Non-Fullerene Acceptors for Organic Solar Cells, *Nat. Rev. Mater.*, 2018, **3**(3), 18003, DOI: 10.1038/natrevmats.2018.3.
- 24 J. Hou, O. Inganäs, R. H. Friend and F. Gao, Organic Solar Cells Based on Non-Fullerene Acceptors, *Nat. Mater.*, 2018, **17**(2), 119–128, DOI: 10.1038/nmat5063.
- 25 S. Li, W. Liu, C.-Z. Li, M. Shi and H. Chen, Efficient Organic Solar Cells with Non-Fullerene Acceptors, *Small*, 2017, **13**(37), 1701120, DOI: 10.1002/sml.201701120.
- 26 J. Zhang, L. Zhu and Z. Wei, Toward Over 15% Power Conversion Efficiency for Organic Solar Cells: Current Status and Perspectives. *Small, Methods*, 2017, **1**(12), 1700258, DOI: 10.1002/smt.201700258.
- 27 A. Venkateswararao, S.-W. Liu and K.-T. Wong, Organic Polymeric and Small Molecular Electron Acceptors for Organic Solar Cells, *Mater. Sci. Eng., R*, 2018, **124**, 1–57, DOI: 10.1016/j.mser.2018.01.001.
- 28 Y. Lin, J. Wang, Z.-G. Zhang, H. Bai, Y. Li, D. Zhu and X. Zhan, An Electron Acceptor Challenging Fullerenes for Efficient Polymer Solar Cells, *Adv. Mater.*, 2015, **27**(7), 1170–1174, DOI: 10.1002/adma.201404317.
- 29 H. Zhang, H. Yao, J. Hou, J. Zhu, J. Zhang, W. Li, R. Yu, B. Gao, S. Zhang and J. Hou, Over 14% Efficiency in Organic Solar Cells Enabled by Chlorinated Nonfullerene Small-Molecule Acceptors, *Adv. Mater.*, 2018, 1800613, DOI: 10.1002/adma.201800613.

- 30 W. Zhao, D. Qian, S. Zhang, S. Li, O. Inganäs, F. Gao and J. Hou, Fullerene-Free Polymer Solar Cells with over 11% Efficiency and Excellent Thermal Stability, *Adv. Mater.*, 2016, **28**(23), 4734–4739, DOI: 10.1002/adma.201600281.
- 31 S. Li, L. Ye, W. Zhao, X. Liu, J. Zhu, H. Ade and J. Hou, Design of a New Small-Molecule Electron Acceptor Enables Efficient Polymer Solar Cells with High Fill Factor, *Adv. Mater.*, 2017, **29**(46), 1704051, DOI: 10.1002/adma.201704051.
- 32 D. Xie, T. Liu, W. Gao, C. Zhong, L. Huo, Z. Luo, K. Wu, W. Xiong, F. Liu and Y. Sun, *et al.*, A Novel Thiophene-Fused Ending Group Enabling an Excellent Small Molecule Acceptor for High-Performance Fullerene-Free Polymer Solar Cells with 11.8% Efficiency, *Sol. RRL*, 2017, **1**(6), 1700044, DOI: 10.1002/solr.201700044.
- 33 A. Wadsworth, M. Moser, A. Marks, M. S. Little, N. Gasparini, C. J. Brabec, D. Baran and I. McCulloch, Critical Review of the Molecular Design Progress in Non-Fullerene Electron Acceptors towards Commercially Viable Organic Solar Cells, *Chem. Soc. Rev.*, 2019, DOI: 10.1039/C7CS00892A.
- 34 Z. Liu, Y. Wu, Q. Zhang and X. Gao, Non-Fullerene Small Molecule Acceptors Based on Perylene Diimides, *J. Mater. Chem. A*, 2016, **4**(45), 17604–17622, DOI: 10.1039/C6TA06978A.
- 35 Y. Duan, X. Xu, Y. Li and Q. Peng, Recent Development of Perylene Diimide-Based Small Molecular Non-Fullerene Acceptors in Organic Solar Cells, *Chin. Chem. Lett.*, 2017, **28**(11), 2105–2115, DOI: 10.1016/j.ccl.2017.08.025.
- 36 C. Li and H. Wonneberger, Perylene Imides for Organic Photovoltaics: Yesterday, Today, and Tomorrow, *Adv. Mater.*, 2012, **24**(5), 613–636, DOI: 10.1002/adma.201104447.
- 37 P. E. Hartnett, A. Timalina, H. S. S. R. Matte, N. Zhou, X. Guo, W. Zhao, A. Facchetti, R. P. H. Chang, M. C. Hersam and M. R. Wasielewski, *et al.*, Slip-Stacked Perylenediimides as an Alternative Strategy for High Efficiency Nonfullerene Acceptors in Organic Photovoltaics, *J. Am. Chem. Soc.*, 2014, **136**(46), 16345–16356, DOI: 10.1021/ja508814z.
- 38 J. Liu, S. Chen, D. Qian, B. Gautam, G. Yang, J. Zhao, J. Bergqvist, F. Zhang, W. Ma and H. Ade, *et al.*, Fast Charge Separation in a Non-Fullerene Organic Solar Cell with a Small Driving Force, *Nat. Energy*, 2016, **1**(7), 16089, DOI: 10.1038/nenergy.2016.89.
- 39 J. Zhang, Y. Li, J. Huang, H. Hu, G. Zhang, T. Ma, P. C. Y. Chow, H. Ade, D. Pan and H. Yan, Ring-Fusion of Perylene Diimide Acceptor Enabling Efficient Nonfullerene Organic Solar Cells with a Small Voltage Loss, *J. Am. Chem. Soc.*, 2017, **139**(45), 16092–16095, DOI: 10.1021/jacs.7b09998.
- 40 Y. Zang, C.-Z. Li, C.-C. Chueh, S. T. Williams, W. Jiang, Z.-H. Wang, J.-S. Yu and A. K.-Y. Jen, Integrated Molecular, Interfacial, and Device Engineering towards High-Performance Non-Fullerene Based Organic Solar Cells, *Adv. Mater.*, 2014, **26**(32), 5708–5714, DOI: 10.1002/adma.201401992.
- 41 D. Sun, D. Meng, Y. Cai, B. Fan, Y. Li, W. Jiang, L. Huo, Y. Sun and Z. Wang, Non-Fullerene-Acceptor-Based Bulk-Heterojunction Organic Solar Cells with Efficiency over 7%, *J. Am. Chem. Soc.*, 2015, **137**(34), 11156–11162, DOI: 10.1021/jacs.5b06414.
- 42 D. Meng, D. Sun, C. Zhong, T. Liu, B. Fan, L. Huo, Y. Li, W. Jiang, H. Choi and T. Kim, *et al.*, High-Performance Solution-Processed Non-Fullerene Organic Solar Cells Based on Selenophene-Containing Perylene Bisimide Acceptor, *J. Am. Chem. Soc.*, 2016, **138**(1), 375–380, DOI: 10.1021/jacs.5b11149.
- 43 H. Langhals and S. Kirner, Novel Fluorescent Dyes by the Extension of the Core of Perylenetetracarboxylic Bisimides, *Eur. J. Org. Chem.*, 2000, **2000**(2), 365–380, DOI: 10.1002/(SICI)1099-0690(200001)2000:2 < 365::AID-EJOC365 > 3.0.CO; 2-R.
- 44 R. K. Gupta, D. S. Shankar Rao, S. K. Prasad and A. S. Achalkumar, Columnar Self-Assembly of Electron-Deficient Dendronized Bay-Annulated Perylene Bisimides, *Chem. – Eur. J.*, 2018, **24**(14), 3566–3575, DOI: 10.1002/chem.201705290.
- 45 Z. Ma, H. Fu, D. Meng, W. Jiang, Y. Sun and Z. Wang, Isomeric *N*-Annulated Perylene Diimide Dimers for Organic Solar Cells, *Chem. – Asian J.*, 2018, **13**(8), 918–923, DOI: 10.1002/asia.201800058.
- 46 F. You, X. Zhou, H. Huang, Y. Liu, S. Liu, J. Shao, B. Zhao, T. Qin and W. Huang, *N*-Annulated Perylene Diimide Derivatives as Non-Fullerene Acceptors for Solution-Processed Solar Cells with an Open-Circuit Voltage of up to 1.14 V, *New J. Chem.*, 2018, **42**(18), 15079–15087, DOI: 10.1039/C8NJ02566E.
- 47 S. V. Dayneko, A. D. Hendsbee and G. C. Welch, Combining Facile Synthetic Methods with Greener Processing for Efficient Polymer-Perylene Diimide Based Organic Solar Cells, *Small Methods*, 2018, **2**(6), 1800081, DOI: 10.1002/smt.201800081.
- 48 S. V. Dayneko, A. D. Hendsbee and G. C. Welch, Fullerene-Free Polymer Solar Cells Processed from Non-Halogenated Solvents in Air with PCE of 4.8%, *Chem. Commun.*, 2017, **53**(6), 1164–1167, DOI: 10.1039/C6CC08939A.
- 49 S. M. McAfee, A.-J. Payne, S. V. Dayneko, G. P. Kini, C. E. Song, J.-C. Lee and G. C. Welch, A Non-Fullerene Acceptor with a Diagnostic Morphological Handle for Streamlined Screening of Donor Materials in Organic Solar Cells, *J. Mater. Chem. A*, 2017, **5**(32), 16907–16913, DOI: 10.1039/C7TA05282K.
- 50 S. M. McAfee, S. V. Dayneko, P. Josse, P. Blanchard, C. Cabanetos and G. C. Welch, Simply Complex: The Efficient Synthesis of an Intricate Molecular Acceptor for High-Performance Air-Processed and Air-Tested Fullerene-Free Organic Solar Cells, *Chem. Mater.*, 2017, **29**(3), 1309–1314, DOI: 10.1021/acs.chemmater.6b04862.
- 51 S. M. McAfee, A.-J. Payne, A. D. Hendsbee, S. Xu, Y. Zou and G. C. Welch, Toward a Universally Compatible Non-Fullerene Acceptor: Multi-Gram Synthesis, Solvent Vapor Annealing Optimization, and BDT-Based Polymer Screening, *Sol. RRL*, 2018, 1800143, DOI: 10.1002/solr.201800143.
- 52 A. D. Hendsbee, J. P. Sun, W. K. Law, H. Yan, I. G. Hill, D. M. Spasyuk and G. C. Welch, Synthesis, Self-Assembly, and Solar Cell Performance of *N*-Annulated Perylene Diimide Non-Fullerene Acceptors, *Chem. Mater.*, 2016, **28**(19), 7098–7109, DOI: 10.1021/acs.chemmater.6b03292.
- 53 Z. Chen, V. Stepanenko, V. Dehm, P. Prins, L. D. A. Siebbeles, J. Seibt, P. Marquetand, V. Engel and F. Würthner, Photoluminescence and Conductivity of Self-Assembled  $\pi$ - $\pi$  Stacks of Perylene Bisimide Dyes, *Chem. – Eur. J.*, 2007, **13**(2), 436–449, DOI: 10.1002/chem.200600889.
- 54 Y. Fan, K. Ziabrev, S. Zhang, B. Lin, S. Barlow and S. R. Marder, Comparison of the Optical and Electrochemical

- Properties of Bi(Perylene Diimide)s Linked through Ortho and Bay Positions, *ACS Omega*, 2017, **2**(2), 377–385, DOI: 10.1021/acsomega.6b00537.
- 55 H. Wang, L. Chen and Y. Xiao, A Simple Molecular Structure of Ortho-Derived Perylene Diimide Diploid for Non-Fullerene Organic Solar Cells with Efficiency over 8%, *J. Mater. Chem. A*, 2017, **5**(42), 22288–22296, DOI: 10.1039/C7TA06804B.
- 56 S. Ghosh, X.-Q. Li, V. Stepanenko and F. Würthner, Control of H- and J-Type  $\pi$  Stacking by Peripheral Alkyl Chains and Self-Sorting Phenomena in Perylene Bisimide Homo- and Heteroaggregates, *Chem. – Eur. J.*, 2008, **14**(36), 11343–11357, DOI: 10.1002/chem.200801454.
- 57 M. Más-Montoya and R. A. J. Janssen, The Effect of H- and J-Aggregation on the Photophysical and Photovoltaic Properties of Small Thiophene-Pyridine-DPP Molecules for Bulk-Heterojunction Solar Cells, *Adv. Funct. Mater.*, 2017, **27**(16), 1605779, DOI: 10.1002/adfm.201605779.
- 58 C. M. Cardona, W. Li, A. E. Kaifer, D. Stockdale and G. C. Bazan, Electrochemical Considerations for Determining Absolute Frontier Orbital Energy Levels of Conjugated Polymers for Solar Cell Applications, *Adv. Mater.*, 2011, **23**(20), 2367–2371, DOI: 10.1002/adma.201004554.
- 59 A. Namepetra, E. Kitching, A. F. Eftaiha, I. G. Hill and G. C. Welch, Understanding the Morphology of Solution Processed Fullerene-Free Small Molecule Bulk Heterojunction Blends, *Phys. Chem. Chem. Phys.*, 2016, **18**(18), 12476–12485, DOI: 10.1039/C6CP01269H.
- 60 D. Zhao, Q. Wu, Z. Cai, T. Zheng, W. Chen, J. Lu and L. Yu, Electron Acceptors Based on  $\alpha$ -Substituted Perylene Diimide (PDI) for Organic Solar Cells, *Chem. Mater.*, 2016, **28**(4), 1139–1146, DOI: 10.1021/acs.chemmater.5b04570.
- 61 R. Singh, S. R. Suranagi, J. Lee, H. Lee, M. Kim and K. Cho, Unraveling the Efficiency-Limiting Morphological Issues of the Perylene Diimide-Based Non-Fullerene Organic Solar Cells, *Sci. Rep.*, 2018, **8**(1), 2849.
- 62 S. Rafique, S. M. Abdullah, K. Sulaiman and M. Iwamoto, Fundamentals of Bulk Heterojunction Organic Solar Cells: An Overview of Stability/Degradation Issues and Strategies for Improvement, *Renewable Sustainable Energy Rev.*, 2018, **84**, 43–53, DOI: 10.1016/j.rser.2017.12.008.
- 63 Y. Sun, J. H. Seo, C. J. Takacs, J. Seifert and A. J. Heeger, Inverted Polymer Solar Cells Integrated with a Low-Temperature-Annealed Sol-Gel-Derived ZnO Film as an Electron Transport Layer, *Adv. Mater.*, 2011, **23**(14), 1679–1683, DOI: 10.1002/adma.201004301.
- 64 A. Sharenko, C. M. Proctor, T. S. van der Poll, Z. B. Henson, T.-Q. Nguyen and G. C. Bazan, A High-Performing Solution-Processed Small Molecule:Perylene Diimide Bulk Heterojunction Solar Cell, *Adv. Mater.*, 2013, **25**(32), 4403–4406, DOI: 10.1002/adma.201301167.
- 65 R. Singh, E. Aluicio-Sarduy, Z. Kan, T. Ye, R. C. I. MacKenzie and P. E. Keivanidis, Fullerene-Free Organic Solar Cells with an Efficiency of 3.7% Based on a Low-Cost Geometrically Planar Perylene Diimide Monomer, *J. Mater. Chem. A*, 2014, **2**(35), 14348–14353, DOI: 10.1039/C4TA02851A.
- 66 A. D. Hendsbee, S. V. Dayneko, J. A. Pells, J. R. Cann and G. C. Welch, N-Annulated Perylene Diimide Dimers: The Effect of Thiophene Bridges on Physical, Electronic, Optical, and Photovoltaic Properties. Sustain, *Energy Fuels*, 2017, **1**(5), 1137–1147, DOI: 10.1039/C7SE00056A.
- 67 J. Cann, S. Dayneko, J.-P. Sun, A. D. Hendsbee, I. G. Hill and G. C. Welch, N-Annulated Perylene Diimide Dimers: Acetylene Linkers as a Strategy for Controlling Structural Conformation and the Impact on Physical, Electronic, Optical and Photovoltaic Properties, *J. Mater. Chem. C*, 2017, **5**(8), 2074–2083, DOI: 10.1039/C6TC05107C.